

Pre-dissolution effect: accelerated contamination of a carbonate aquifer by mine waters*

Yevhen Vasylenko

January 3, 2026

Abstract

High-salinity mine water infiltration into carbonate aquifers may enhance contaminant migration due to the pre-dissolution of carbonate minerals. This short article presents the results of PHREEQC thermodynamic modeling of the Svystunova Gully mine water impoundment (Ukraine). The calculations demonstrate that aggressive mine waters, initially undersaturated with respect to carbonates, induce local dissolution, thereby potentially increasing permeability. This, in turn, further accelerates the spread of contamination. Pre-dissolution is therefore identified as a key mechanism explaining both the intensity and extent of groundwater contamination in carbonate environments.

Keywords: mine water, carbonate aquifer, thermodynamic modeling, PHREEQC, pre-dissolution effect, mixing corrosion, infiltration metasomatism.

1 Introduction

The mine water impoundment in Svystunova Gully, designed to store highly mineralized mine waters, was constructed in 1975. Initially, it was intended as a temporary solution. The design capacity of the impoundment is 14 million m^3 . Paradoxically, the facility has not yet been legally commissioned and is officially classified as an object of incomplete construction, which, however, has not prevented its actual operation for half a century.

*DOI: 10.5281/zenodo.18142106

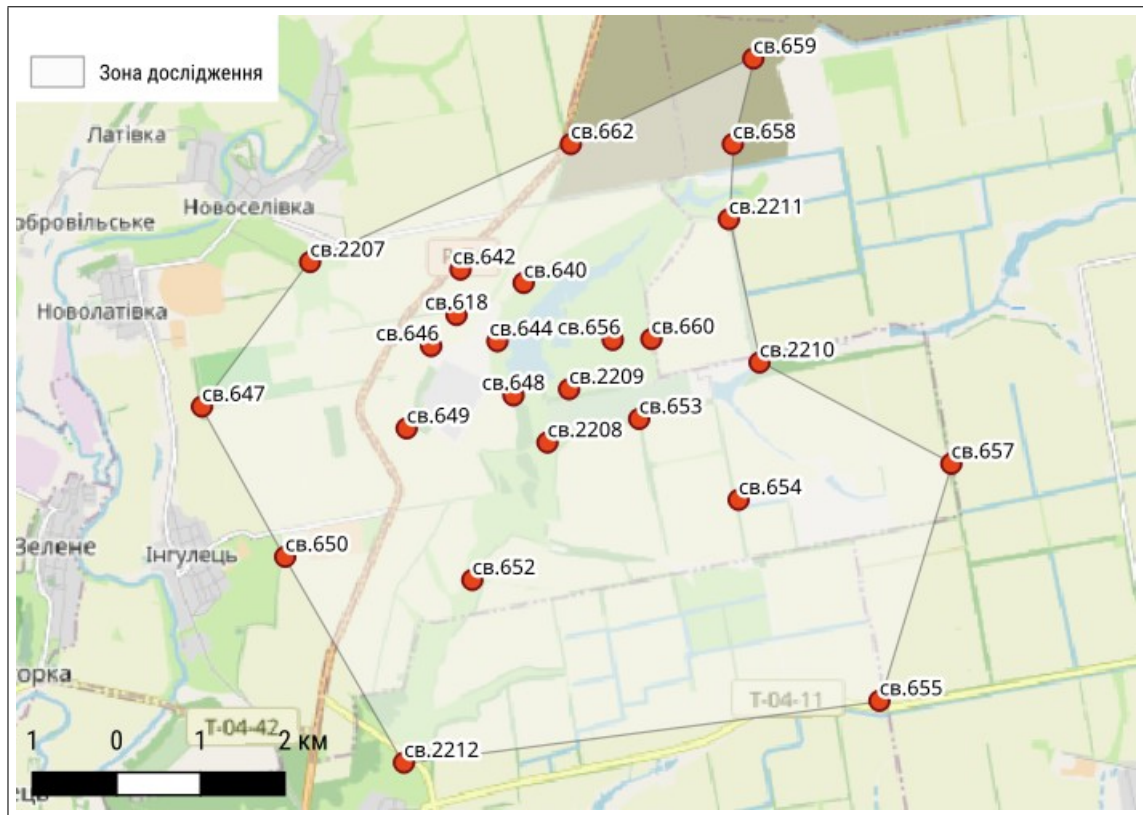


Figure 1: General layout of the mine water impoundment, monitoring well network, and the results interpretation zone («СВ.618»–«СВ.2212» — monitoring wells)

Immediately after the initial filling of the impoundment, leakage into the underlying groundwater horizon began. The aquifer is confined to Neogene sands and limestones (with a significant predominance of the latter). Cases of catastrophic leakage have been recorded—likely into subsurface karst voids—where the impoundment drained completely [16, p. 176]. Literature sources also mention another accident involving the loss of approximately 8 million m^3 of water, resulting in the formation of suffusion-karst sinkholes in the compacted clay liner [8, p. 122].

The general layout of the mine water impoundment, the network of monitoring wells, and the interpretation zone for the obtained results are shown in Figure 1. While more wells exist, only those providing data used in this study are displayed. Some of the omitted wells are abandoned or clogged, while others are designated for monitoring the Quaternary aquifer, which is virtually unaffected by the facility in question.

Over the operational period of the impoundment, an extensive multi-kilometer contamination plume has formed in the surrounding rocks, leading to significant alterations in groundwater composition. In the last decade, the impoundment has received 10–13 million m^3 of mine water annually, with an average mineralization of 28–38 g/L. The waters are predominantly chloride magnesium-sodium type. During the cold season, the accumulated waters are discharged into the Inhulets River.

The management scheme for highly mineralized mine waters in the Kryvyi Rih Iron Ore Basin is a complex multi-stage mechanism involving numerous intermediate links: mine water collection by drainage systems, transport to intermediate storage and mixing, delivery to the impoundment, losses from the impoundment into the aquifer, discharge into the Inhulets River, and dilution directly within the river channel. The ecological risks and long-term consequences of this management scheme have not yet been fully studied. This research focuses solely on the behavior of leaked mine waters within the underlying aquifer.

2 Methods

Monitoring data (chemical water analyses) from 2012–2021 and March 2022 were used to model the behavior of mine waters in the aquifer. The consolidated dataset was evaluated for errors and inconsistencies; water samples with unresolvable errors were excluded from further processing. General statistical indicators of water chlorinity are presented in Table 1.

Based on the monitoring data, a cycle of thermodynamic modeling was performed using equilibrium thermodynamics methods implemented in the PHREEQC 3.7.3 software package [5, 2]. The ‘minteq.v4.dat’ database was selected; this database is ported from MINTEQA2, another widely used thermodynamic modeling package [1, 4].

It should be noted that water mineralization in the impoundment and the nearest wells ranges from 30 to 40 g/L. This raises questions about the appropriateness of the thermodynamic database selection, as these mineralization values are at the limit of the theoretical validity of the Davies equation. However, a verification of calcite saturation indices (as the main rock-forming mineral) using the ‘pitzer.dat’ database showed negligible discrepancies in the results. Furthermore, the ‘minteq.v4.dat’ database is widely used in calculations of toxic trace element migration, allowing the use of an accumulated empirical base for comparison with the situation in the studied aquifer. The results of the check for discrepancies in calcite saturation indices are shown in Figure 2.

Table 1: Descriptive statistics of Cl^- concentrations in the discharge pipe, mine water impoundment, and monitoring wells

	Sampling Location	Min	Max	Q1	Med	Q3	Mean	Skew	Kurt	N
1	Well 2207	6352	14090	8930	10473	13079	10665	0.02	-1.4	34
2	Well 2208	157	16898	13995	15015	15287	14483	-4.84	25.9	42
3	Well 2209	6686	10275	7343	7976	8906	8122	0.46	-0.7	41
4	Well 2210	576	1223	900	982	1012	973	-0.60	1.8	41
5	Well 2211	532	1087	669	719	914	771	0.41	-0.9	42
6	Well 2212	149	2170	194	219	376	314	5.16	28.1	42
7	Well 618	16187	23308	17228	20028	21662	19457	-0.03	-1.6	39
8	Well 640	866	17407	1804	2314	3304	4394	1.68	1.3	41
9	Well 642	967	14173	1526	1838	3319	2992	2.37	5.7	41
10	Well 644	3382	20201	10566	14361	18420	13488	-0.56	-0.9	42
11	Well 646	800	18833	2060	13705	15189	10004	-0.32	-1.6	42
12	Well 647	1543	3319	1950	2067	2304	2208	1.26	0.7	41
13	Well 648	9659	19064	13470	16058	17190	15352	-0.58	-0.6	40
14	Well 649	5197	19321	11585	12157	12762	12148	0.10	9.5	40
15	Well 650	168	4160	643	1184	1911	1410	1.18	1.0	41
16	Well 652	5775	10280	8284	8971	9287	8705	-1.14	1.2	41
17	Well 653	1144	1964	1462	1596	1660	1568	-0.37	0.8	41
18	Well 654	2858	4458	3424	3741	3981	3678	-0.33	-0.5	39
19	Well 655	714	1184	790	839	874	848	1.64	3.4	40
20	Well 656	9233	24240	14012	17006	20953	17371	0.10	-1.1	40
21	Well 657	828	1180	984	1014	1093	1034	-0.17	-0.2	41
22	Well 658	789	23278	1894	1972	2111	2539	5.50	28.5	34
23	Well 659	58	11645	536	548	584	872	5.45	27.8	33
24	Well 660	3036	6204	3423	3591	3867	3738	2.69	7.7	41
25	Well 662	667	2051	1531	1678	1943	1630	-1.32	1.0	19
26	Impoundment	15977	22419	19492	19893	20883	20034	-0.74	1.7	41
27	Discharge pipe	15948	22069	18387	19604	19923	19406	0.08	-0.1	41

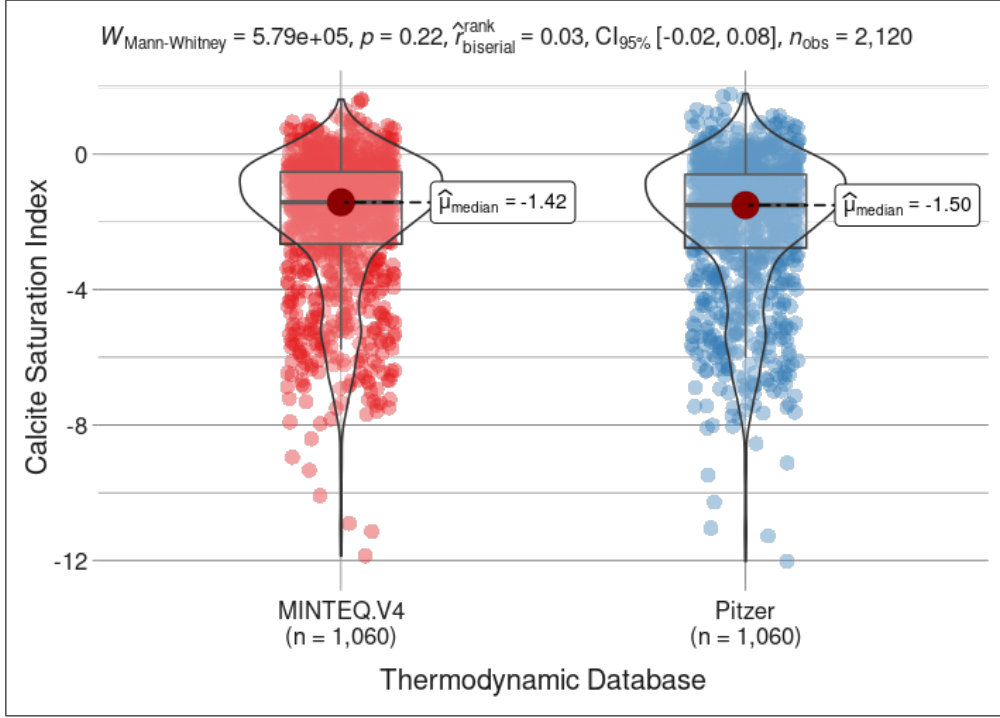


Figure 2: Statistical significance test of differences in calcite saturation indices for MINTEQ and Pitzer databases

Since the primary dataset includes over 1000 individual chemical water analyses, the PHREEQC output files represent a significant volume of data. To convert this into a tabular format, a parser was written in the R programming language [6], which translated the entire text dataset into separate thematic tables (Distribution of species, Saturation indices, Description of solution). To control the parser's output, results were compared with selected indicators exported directly to a table (PHREEQC Selected Output function). This approach allows for the analysis of the entire connected dataset, which is particularly important when modeling the propagation of individual contaminant components.

The dilution coefficient of the leaked mine water by the aquifer water was used as an indicator of "distance" from the impoundment. This choice is dictated by the significant anisotropy of the limestone massif's permeability, likely due to its block structure and predominantly fracture-based permeability. The formula for calculating the dilution coefficient is as follows:

$$P_{\text{fresh}} = \frac{C_{\text{saline}} - C_{\text{mix}}}{C_{\text{saline}} - C_{\text{fresh}}} \quad (1)$$

where:

P_{fresh} — fraction of fresh water in the mixed water body;

C_{saline} — chloride concentration in highly mineralized water prior to mixing with fresh water (median value for the mine water impoundment), mg/L;

C_{fresh} — chloride concentration in fresh water prior to mixing (median value for Well 2212), mg/L;

C_{mix} — chloride concentration in the mixed water (actual value in each water sample), mg/L.

It is important to note that water from Well 2212 is not truly background, as it has also undergone anthropogenic transformation. However, no other data on the primary composition of the aquifer water are available to the author. Descriptive statistics of the dilution coefficient for each monitoring well are given in Table 2.

The variability in water composition and dilution coefficient in each well is evidently linked to the variability in the composition of mine waters entering and filtering from the impoundment.

3 Results

Descriptive statistics of calcite saturation indices are presented in Table 3.

As can be seen from Table 3, the long-term median value of the calcite saturation index is negative in all monitoring wells. This suggests that the system as a whole is aggressive towards limestones. The dependence of the saturation index of carbonate minerals on the distance from the mine water impoundment (dilution coefficient) is shown in Figure 3.

As shown in Figure 3, a clear zonation is observed in the behavior of saturation indices for calcite and other carbonate minerals. The author attributes the existence of an internal aggressive zone (low dilution coefficient values) to the primary aggressiveness of the highly mineralized mine waters towards carbonate minerals. This is followed by a zone of gradual neutralization. At dilution coefficient values of 0.8–0.9, a sharp decrease in carbonate saturation indices is observed. The author associates this phenomenon with the onset of the Mixing Corrosion effect. Unfortunately, monitoring of the aquifer state at greater distances is not performed.

The author hypothesizes that beyond the boundary of the monitoring zone, processes of limestone dolomitization occur [7]. It is worth specifically mentioning that the author considers the entire system of mine water ingress and propagation in the aquifer as a special case of a metasomatic process, in accordance with the theory of D.S. Korzhinsky [12, 3, 13, 14, 15, 10, 11, 9].

Table 2: Descriptive statistics of dilution indices in the discharge pipe, mine water impoundment, and monitoring wells

	Sampling Location	Min	Max	Q1	Med	Q3	Mean	Skew	Kurt	N
1	Well 2207	0.29	0.69	0.35	0.48	0.56	0.47	-0.03	-1.35	34
2	Well 2208	0.15	1.00	0.23	0.25	0.30	0.27	4.81	25.68	42
3	Well 2209	0.49	0.67	0.56	0.61	0.64	0.60	-0.47	-0.76	41
4	Well 2210	0.95	0.98	0.96	0.96	0.97	0.96	0.27	0.08	41
5	Well 2211	0.96	0.98	0.96	0.97	0.98	0.97	-0.23	-1.58	42
6	Well 2212	0.90	1.00	0.99	1.00	1.00	0.99	-5.32	29.28	42
7	Well 618	0.00	0.19	0.00	0.00	0.14	0.07	0.43	-1.57	39
8	Well 640	0.13	0.97	0.84	0.89	0.92	0.79	-1.68	1.25	41
9	Well 642	0.29	0.96	0.84	0.92	0.93	0.86	-2.39	5.86	41
10	Well 644	0.00	0.84	0.07	0.28	0.47	0.33	0.57	-0.91	42
11	Well 646	0.05	0.97	0.24	0.32	0.91	0.50	0.31	-1.62	42
12	Well 647	0.84	0.93	0.89	0.91	0.91	0.90	-1.16	0.41	41
13	Well 648	0.04	0.52	0.14	0.20	0.32	0.23	0.57	-0.62	40
14	Well 649	0.03	0.75	0.36	0.40	0.42	0.39	-0.05	9.66	40
15	Well 650	0.80	1.00	0.91	0.95	0.98	0.94	-1.23	1.15	41
16	Well 652	0.49	0.72	0.54	0.56	0.59	0.57	1.18	1.19	41
17	Well 653	0.91	0.95	0.93	0.93	0.94	0.93	-0.03	1.24	41
18	Well 654	0.78	0.87	0.81	0.82	0.84	0.82	0.27	-0.55	39
19	Well 655	0.95	0.97	0.97	0.97	0.97	0.97	-2.54	5.89	40
20	Well 656	0.00	0.54	0.00	0.15	0.30	0.16	0.40	-1.05	40
21	Well 657	0.95	0.97	0.96	0.96	0.96	0.96	-0.72	0.37	41
22	Well 658	0.00	0.97	0.90	0.91	0.91	0.89	-5.46	28.28	34
23	Well 659	0.42	1.00	0.98	0.98	0.98	0.96	-5.45	27.85	33
24	Well 660	0.70	0.86	0.81	0.83	0.84	0.82	-2.58	7.32	41
25	Well 662	0.91	0.98	0.91	0.93	0.93	0.93	1.45	1.32	19
26	Impoundment	0.00	0.20	0.00	0.00	0.02	0.02	3.26	10.56	41
27	Discharge pipe	0.00	0.20	0.00	0.01	0.08	0.04	1.13	0.72	41

Table 3: Descriptive statistics of calcite saturation indices in the discharge pipe, mine water impoundment, and monitoring wells

	Sampling Location	Min	Max	Q1	Med	Q3	Mean	Skew	Kurt	N
1	Well 2207	-5.48	0.84	-3.01	-1.92	-1.02	-1.96	-0.26	-0.69	34
2	Well 2208	-4.62	0.90	-2.16	-1.23	-0.02	-1.12	-0.38	-0.18	42
3	Well 2209	-4.14	1.03	-1.41	-0.88	-0.56	-1.05	-0.93	2.09	41
4	Well 2210	-9.34	-0.25	-3.45	-2.15	-1.23	-2.94	-1.24	0.95	41
5	Well 2211	-5.42	-0.31	-2.44	-1.81	-1.16	-1.87	-0.97	1.70	42
6	Well 2212	-5.77	0.15	-2.35	-1.83	-1.19	-1.87	-0.99	2.42	42
7	Well 618	-11.87	-0.63	-5.34	-4.35	-2.88	-4.49	-0.94	1.25	39
8	Well 640	-6.87	0.73	-3.45	-1.60	-0.77	-2.16	-0.67	-0.67	41
9	Well 642	-10.91	1.63	-6.23	-4.54	-0.42	-3.55	0.03	-1.17	41
10	Well 644	-4.85	0.73	-1.55	-0.79	-0.30	-1.18	-1.27	0.82	42
11	Well 646	-7.59	0.32	-4.00	-1.46	-0.79	-2.37	-0.93	-0.34	42
12	Well 647	-11.15	-3.39	-6.69	-6.12	-5.13	-6.02	-0.88	3.35	41
13	Well 648	-5.76	-0.03	-3.03	-1.69	-0.74	-2.18	-0.75	-0.64	40
14	Well 649	-2.09	1.10	-0.97	-0.40	0.07	-0.42	-0.25	-0.52	40
15	Well 650	-6.71	-0.18	-3.81	-2.31	-1.34	-2.72	-0.72	-0.43	41
16	Well 652	-3.64	1.14	-1.77	-1.21	0.26	-0.99	-0.02	-1.11	41
17	Well 653	-3.30	0.44	-2.05	-1.50	-0.54	-1.38	-0.13	-1.03	41
18	Well 654	-2.39	0.99	-1.52	-0.98	-0.11	-0.83	0.06	-1.10	39
19	Well 655	-3.99	0.69	-1.67	-0.58	-0.30	-1.03	-0.80	-0.09	40
20	Well 656	-7.25	-0.74	-4.21	-3.06	-1.75	-3.24	-0.51	-0.66	40
21	Well 657	-3.86	0.01	-2.10	-1.65	-1.02	-1.61	-0.52	0.28	41
22	Well 658	-6.51	0.18	-5.09	-3.00	-2.01	-3.25	-0.17	-0.99	34
23	Well 659	-6.01	0.30	-2.22	-1.59	-1.32	-1.84	-1.63	4.55	33
24	Well 660	-2.30	0.72	-1.02	-0.40	0.06	-0.52	-0.39	-0.41	41
25	Well 662	-1.65	0.46	-1.08	-0.56	-0.40	-0.65	0.03	-0.69	19
26	Impoundment	-2.10	1.30	-0.47	-0.33	0.15	-0.21	-0.28	2.34	41
27	Discharge pipe	-2.07	0.56	-0.65	-0.41	-0.08	-0.36	-0.41	0.92	41

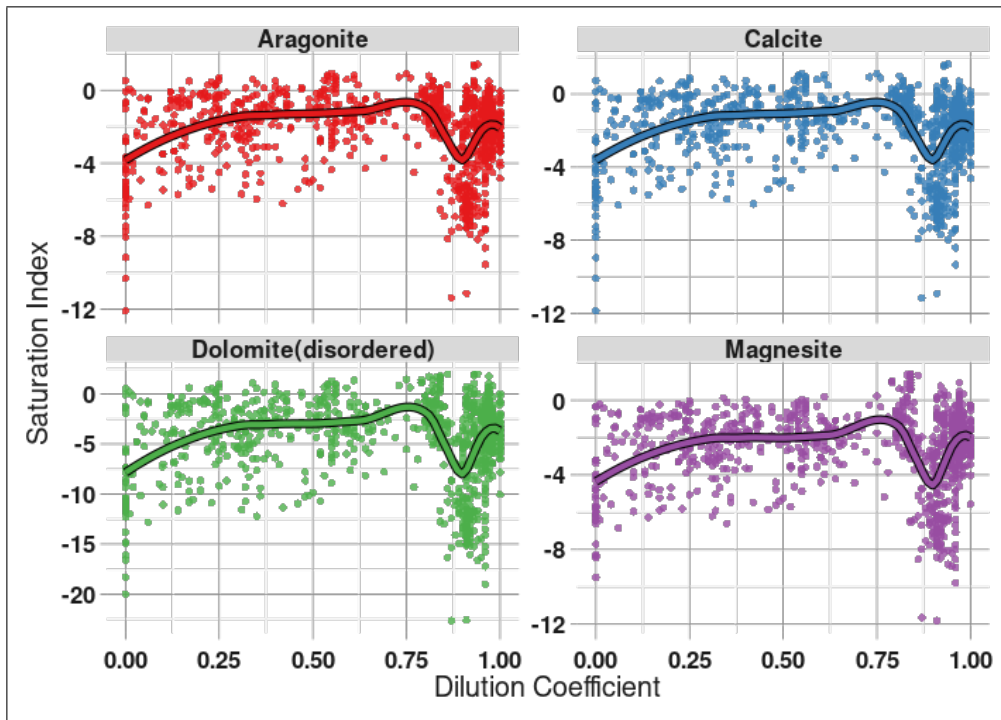


Figure 3: Dependence of saturation indices of major carbonate minerals on the dilution coefficient of leaked high-salinity waters. Trend lines represent robust locally estimated scatterplot smoothing (LOESS) with a span of 0.5

Consequently, this process is governed by the laws of infiltration metasomatic zoning and can lead to the formation of a specific type of anthropogenic metasomatic zonation [7].

4 Conclusion

Modeling results indicate that mine waters are initially undersaturated with respect to carbonate minerals. This causes aggressive dissolution of the limestone matrix in the immediate vicinity of the mine water impoundment. As mine waters advance through the aquifer, they gradually lose aggressiveness and nearly reach equilibrium with carbonate minerals. However, within the outer contour of the contamination plume, the Mixing Corrosion mechanism is triggered, leading to a renewed dissolution of limestones.

Such "dual-zone" rock dissolution may result in the outer dissolution zone "preparing the pathways" for the subsequent influx of new contaminant portions from the inner zone. Thus, a positive feedback system is formed. The danger of such synergy lies in the fact that even in the event of complete isolation of leakages from the impoundment, it will not be possible to halt the dissolution process of the limestone massif: in the absence of new portions of highly mineralized water, the outer dissolution zone will simply begin to advance inwards into the contamination plume due to the gradual dilution of the mine waters remaining in the rock massif.

This study represents a condensed summary of the research findings detailed in the author's monograph [7]. For a more comprehensive analysis of the hydrogeochemical data, thermodynamic modeling parameters, and the theoretical basis of the metasomatic approach, readers are referred to this publication <https://doi.org/10.5281/zenodo.16741148>.

References

- [1] Jerry Allison, D. Brown, and K. Novo-Gradac. *MINTEQA2/PRODEFA2, a geochemical assessment model for environmental systems: Version 3. 0 user's manual*, 01 1991.
- [2] S. R. Charlton and D. L. Parkhurst. Modules based on the geochemical model PHREEQC for use in scripting and programming languages. *Computers & Geosciences*, 37(10):1653–1663, October 2011.

- [3] D. S. Korzhinskii. The theory of systems with perfectly mobile components and processes of mineral formation. *American Journal of Science*, 263(3):193–205, March 1965.
- [4] D. Langmuir. *Aqueous Environmental Geochemistry*. Prentice Hall, New Jersey, 1997.
- [5] D. L. Parkhurst and C. A. J. Appelo. *Description of input and examples for PHREEQC version 3—A computer program for speciation, batch-reaction, one-dimensional transport, and inverse geochemical calculations*, 2013.
- [6] R Core Team. *R: A Language and Environment for Statistical Computing*. R Foundation for Statistical Computing, Vienna, Austria, 2024.
- [7] Yevhen Vasylenko. *Hydrogeochemical modeling of the impact of filtration loss of highly mineralized mine water from the storage pond in the Svystunova gully: version 0.75 (Ukrainian)*. Zenodo, 2025.
- [8] Г. Н. Дублянская and В. Н. Дублянский. *Картографирование, районирование и инженерно-геологическая оценка закарстованных территорий*. Издательство Объединённого института геологии, геофизики и минералогии Сибирского отделения российской академии наук, 1992.
- [9] В. А. Жариков, В. Л. Русинов, А. А. Маракушев, Г. П. Зарайский, Б. И. Омеляненко, Н. Н. Перцев, И. Т. Расс, О. В. Андреева, С. С. Абрамов, and К. В. Подлесский. *Метасоматизм и метасоматические породы*. Научный мир, Москва, 1998.
- [10] Г. П. Зарайский. *Зональность и условия образования метасоматических пород*. Наука, Москва, 1989.
- [11] Г. П. Зарайский. *Эксперимент в решении проблем метасоматизма*. Серия «Чтения имени академика Д. С. Коржинского». ГЕОС, Москва, 2007.
- [12] Д. С. Коржинский. Очерк метасоматических процессов. In А. Г. Бетехтин, Ф. И. Вольфсон, А. Н. Заварицкий, Д. С. Коржинский, О. Д. Левицкий, and В. А. Николаев, editors, *Основные проблемы в учении о магматогенных рудных месторождениях. Второе издание*, pages 334–456, Москва, 1955. Академия наук СССР, Институт геологических наук, Издательство Академии наук СССР.

- [13] Д. С. Коржинский. *Теория метасоматической зональности*. Наука, Москва, 1969.
- [14] Д. С. Коржинский. *Теория метасоматической зональности*. Наука, Москва, 2-е, дополненное edition, 1982.
- [15] Д. С. Коржинский. *Избранные труды: Основы метасоматизма и метамагматизма*. Наука, Москва, 1993.
- [16] Е. Ф. Шнюков, В. М. Шестопапов, Е. А. Яковлев, В. Н. Бабиченко, and Р. А. Баер. *Экологическая геология Украины. Справочное пособие*. Наукова Думка, Киев, 1993.